

Designing Inherently Photodegradable Cell-Adhesive Hydrogels for 3D Cell Culture

Alisa Rosenfeld, Tobias Göckler, Mariia Kuzina, Markus Reischl, Ute Schepers, and Pavel A. Levkin*

Light-based microfabrication techniques constitute an indispensable approach to fabricate tissue assemblies, benefiting from noncontact spatially and temporarily controlled manipulation of soft matter. Light-triggered degradation of soft materials, such as hydrogels, is important in tissue engineering, bioprinting, and related fields. The photoresponsiveness of hydrogels is generally not intrinsic and requires complex synthetic procedures wherein photoresponsive crosslinking groups are incorporated into the hydrogel. This paper demonstrates a novel biocompatible and inherently photodegradable poly(ethylene glycol) methacrylate (PEGMA)-based gelatin-methacryloyl (GelMA)-containing hydrogel that can be used to culture cells in 3D for at least 14 d. These gels are conveniently and quickly degraded via UV irradiation for 10 min to produce structured hydrogels of various geometries, sizes, and free-standing cell-laden hydrogel particles. These structures can be flexibly produced on demand. In particular, photodegradation can be temporarily delayed from photopolymerization, offering an alternative to hydrogel array production via photopolymerization with a photomask. The paper investigates the influences of hydrogel composition and swelling liquid on both its photodegradability and biocompatibility.


their responsive properties. Hydrogel design has sought to make hydrogels accessible for a variety of stimuli capable of either synthesizing^[1,2] the hydrogel or inducing changes (e.g., degradation,^[3] drug release,^[4] and sol-gel transition^[5]) in hydrogels. Certain stimuli, including enzymes,^[6] pH,^[7] and small molecules such as glucose,^[8] induce responses via direct molecular contact with a hydrogel or its precursors. Other stimuli, such as temperature^[7] and light,^[9] enable synthesis and manipulation of soft matter in a noncontact spatiotemporal manner, which is why stimuli have become increasingly important in biological settings. Photopolymerization and photodegradation are especially noteworthy given their high tunability of wavelength and intensity; the use of photomasks also enables sharp control of spatial resolution. Apart from the spatial control over the features, the potential biological applications of photodegradable hydrogels include the manipulation of the mechanical properties for dynamic cell culture studies, release of incorporated molecules (proteins, enzymes, drugs etc.) and others.

Usually, hydrogels can be made photodegradable through additional functionalization with photoresponsive groups that must be incorporated into the hydrogel network and act as fracture points for light. Various photolabile groups can be introduced into hydrogels; the most common one is the *o*-nitrobenzylester

1. Introduction

Responsiveness is a ubiquitous property of biological systems and a primary characteristic of living matter. To mimic living systems more effectively, extensive research has been devoted to hydrogels that resemble biological systems based on

Dr. A. Rosenfeld, M. Kuzina, Prof. P. A. Levkin
Institute of Biological and Chemical Systems - Functional Molecular Systems (IBCS-FMS)
Karlsruhe Institute of Technology (KIT)
Hermann-von-Helmholtz-Platz 1, Eggenstein-Leopoldshafen 76344, Germany
E-mail: levkin@kit.edu

 The ORCID identification number(s) for the author(s) of this article can be found under <https://doi.org/10.1002/adhm.202100632>

© 2021 The Authors. Advanced Healthcare Materials published by Wiley-VCH GmbH. This is an open access article under the terms of the Creative Commons Attribution-NonCommercial License, which permits use, distribution and reproduction in any medium, provided the original work is properly cited and is not used for commercial purposes.

DOI: 10.1002/adhm.202100632

Dr. T. Göckler, Prof. U. Schepers
Institute of Functional Interfaces (IFG)
Karlsruhe Institute of Technology (KIT)
Hermann-von-Helmholtz-Platz 1, Eggenstein-Leopoldshafen 76344, Germany
Prof. M. Reischl
Institute for Automation and Applied Informatics (IAI)
Karlsruhe Institute of Technology (KIT)
Hermann-von-Helmholtz-Platz 1, Eggenstein-Leopoldshafen 76344, Germany
Prof. U. Schepers, Prof. P. A. Levkin
Institute of Organic Chemistry
Karlsruhe Institute of Technology (KIT)
Karlsruhe 76131, Germany

group,^[10–12] although other groups^[13] such as coumarin,^[14] disulfides,^[15] and ruthenium (II) polypyridyl complexes^[16] are also used. Sophisticated *o*-nitrobenzyl derivatives of gelatin can be utilized to support cell adhesion to yield matrices for 3D cell cultures.^[17,18] Despite many accomplishments in this field, the limited number of photolabile moieties and associated synthetic challenges greatly constrain the monomers that can be used in synthesis. Flexibility and heterogeneity are needed to more accurately mimic complex biological systems. Also, highly simplified synthetic procedures are essential for the rapid development of nature-like hydrogels. Thus, cell-compatible inherently photodegradable hydrogels produced from simple, widely accessible monomers are needed.

Recently, we demonstrated the inherent photodegradability of poly(ethylene glycol) methacrylate (PEGMA)-based hydrogels.^[3] The remarkable minute-scale photodegradability of PEGMA hydrogels is attributable to the combination of inherent photodegradability of polymethacrylates, UV transparency of water, and strong swelling of the hydrogel network. The increased interpolymer chain distance in the swollen hydrogel and high volumes of solvent between the polymer chains lead to the domination of chain scission and degradation over recrosslinking reactions (Figure S3, Supporting Information). UV degradability is thus associated with hydrogel swellability, which can be influenced by, e.g., introducing charged monomers.^[19] These photopolymerizable, inherently photodegradable PEGMA-based hydrogels are biologically inert and nontoxic, similar to other PEG-based hydrogels, but lack cell adhesion and enzymatic degradation sites. By contrast, gelatin-methacryloyl (GelMA) displays excellent biocompatibility and biodegradability and can be conveniently photopolymerized.^[20–23] However, GelMA substantially reduces the swelling ability of poly(ethylene glycol) dimethacrylate (PEGDMA) hydrogels because of its interaction with PEG.^[24] One of the photodegradation mechanisms via formation of formyl radicals is less accessible for amides due to partial double bond character of the carbon–nitrogen bond in amides. Since methacrylate groups are tethered to gelatin's backbone via amide bonds, their photomediated scission is less favorable than ester-bound methacrylate groups in PEGMA. Furthermore, the aromatic amino acids of gelatin absorb UV light at 280 nm, thereby reducing its effective intensity (Figure S4, Supporting Information); therefore, gelatin-based polymethacrylates do not demonstrate photodegradable behavior compared to PEG-based methacrylate hydrogels. Overall, we hypothesize that supplementing PEGMA hydrogels with low concentrations of GelMA can enhance the hydrogels' cell encapsulation ability while retaining photodegradation properties.

The aim of this study was to develop a biocompatible, easily accessible, photopolymerizable, and photodegradable material for 3D cell culture millimeter-scale structuring. This synthetic challenge was addressed by constructing a combinatorial library of PEGMA/PEGDMA/GelMA hydrogels and investigating how the addition of GelMA influenced the photodegradation properties of PEG-based hydrogels (i.e., the structure-function relationship). The formulation with the fastest degradability was tested on three cell types and demonstrated good cell viability. The kinetics of photodegradation were evaluated, and customizable 3D cell cultures (e.g., hydrogel micropad arrays) were generated in a proof-of-concept fabrication.

2. Experimental Section

Lithium phenyl(2,4,6-trimethylbenzoyl)phosphinate (LAP) was purchased from TCI Chemicals Deutschland (Eschborn, Germany). Dulbecco's phosphate buffered saline (DPBS), Dulbecco's modified Eagle medium (DMEM), fetal calf serum (FCS), penicillin-streptomycin, and calcein-AM were purchased from Gibco Life Technologies (Carlsbad, USA). The CellTiter 96 nonradioactive cell proliferation assay (MTT) was purchased from Promega GmbH (Mannheim, Germany). Dialysis tubes (MWCO 12–14 kDa) were obtained from VWR International GmbH (Darmstadt, Germany). All other chemicals were purchased from Sigma-Aldrich Chemie (Steinheim, Deutschland). Normal human dermal fibroblasts (NHDF), human liver cancer cells (HepG2), and HeLa cells were purchased from PromoCell GmbH (Heidelberg, Germany). PrestoBlue cell viability reagent was purchased from Thermo Fischer Scientific.

2.1. Synthesis of Water-Soluble Photoinitiator

Sodium phenyl(2,4,6-trimethylbenzoyl)phosphinate (SAP) was used in cell-free experiments due to its enhanced solubility in water and was synthesized as follows. Ethyl (2,4,6-trimethylbenzoyl)phenylphosphinate (1 g, 0.003 mol) was dissolved in 10 mL 2-butanone, to which sodium iodide (0.6 g, 0.004 mol) was added. The reaction mixture was stirred overnight at 60 °C. The precipitate was then filtered off, washed with 2-butanone, and dried. Sodium phenyl(2,4,6-trimethylbenzoyl)phosphinate (yield: 0.7 g, 79%) was yielded as a white solid.

¹H NMR (400 MHz, D₂O): δ /ppm = 7.78–7.48 (H_{aromatic}, phenyl), 6.92 (s, H_{aromatic}, benzoyl), 2.27 (s, para-CH₃), 2.06 (s, ortho-CH₃) (Figure S1, Supporting Information).

2.2. Synthesis of Gelatin-Methacryloyl (GelMA)

The synthesis and purification of gelatin-methacryloyl (GelMA) were performed as previously described in literature.^[21,23] In brief, 1 g gelatin (type A, gel strength \approx 300 g bloom, 0.266 mmol NH₂ groups, 1 equiv.) was dissolved in 10 mL DPBS, and the solution was heated to 50 °C. After complete dissolution of gelatin, 39.6 μ L methacrylic anhydride (0.266 mmol, 1 equiv.) was added dropwise and the reaction mixture was stirred at 50 °C for 2 h. Next, the solution was diluted with 10 mL dH₂O, transferred into dialysis tubes (MWCO: 12–14 kDa), and dialyzed against dH₂O at 40 °C for 7 d. The purified solution was frozen at –80 °C and lyophilized (Lyophilisator Christ Alpha 1-4 Christ Gefriertrocknungsanlagen GmbH, Osterode am Harz, Germany). The product was obtained as a white solid and stored at –20 °C. GelMA with various degrees of functionalization (low, medium, or high) was obtained by varying the amount of methacrylic anhydride (1 equiv., 8 equiv., 20 equiv. referred to NH₂ groups in gelatin).

¹H NMR (400 MHz, D₂O): δ /ppm = 7.46–7.22 (H_{aromatic}, gelatin), 5.73 (H_{vinyl}), 5.48 (H_{vinyl}), 5.08–0.83 (gelatin), 3.04 (bs, NH₂), 1.95 (s, CH₃) (Figure S2, Supporting Information).

2.3. Nuclear Magnetic Resonance Spectroscopy

Nuclear magnetic resonance measurements were performed using a 400 MHz NMR spectrometer (AVANCE 400; Bruker, Rheinstetten, Germany). Chemical shifts are given in parts per million (δ /ppm) downfield from tetramethylsilane (TMS) and referenced to D₂O (4.80 ppm) as internal standard. In the description of signals, s = singlet and bs = broad singlet. ¹H NMR spectra of gelatin and GelMA were recorded at a temperature of 315 K to avoid gelation of the sample during the measurement.

2.4. 2,4,6-Trinitrobenzene Sulfonic Acid Assay

The percentage of modified free amino groups in GelMA was determined colorimetrically by a TNBSA assay. The TNBSA assay was performed according to an established protocol using protein solutions of 500 $\mu\text{g mL}^{-1}$ gelatin and GelMA (low, medium, or high), respectively.^[25] For each blank, the protein solutions were first mixed with HCl before adding the TNBSA reagent. The absorption of each sample was measured at 335 nm (SmartSpec 3000, Bio-Rad Laboratories GmbH, Munich Germany) All measurements were performed in triplicate. The degree of functionalization (DoF) was calculated from the ratio of the absorption values of functionalized and non-functionalized gelatin.

$$\text{DoF [\%]} = \left(1 - \frac{A(\text{GelMA})}{A(\text{gelatin})} \right) \times 100\% \quad (1)$$

2.5. Combinatorial Library Synthesis

Monomers were de-inhibited prior to use by passing over a short column of basic aluminum oxide from Alfa Aesar (Ward Hill, Massachusetts, USA). Each prepolymerization mixture (240 μL) according to the scheme (Figure 1) was deposited into a silicone mold (14 mm \times 5 mm \times 3 mm) and subsequently photopolymerized with UV light (360 nm, 6 mW cm^{-2}) for 2 min. The photodegradation of each hydrogel was assessed by weighing the hydrogel before and after irradiation under UV light (270 nm, 22 mW cm^{-2}); excess released liquid was removed prior to weighing. Combinations 1–29 were synthesized in batches (1–9, 10–17, 18–20, 21–25, 26–29) and used one after another for improving the mathematic approximation, whereas combinations 30–32 were used to validate the resulting model.

In order to determine the degradation behavior of hydrogels with different thicknesses, hydrogels in varying volumes (80, 120, and 180 μL) were polymerized in a silicone mold for 2 min (360 nm, 6 mW cm^{-2}). After swelling in DMEM lacking phenol red and FCS, the hydrogels in triplicates were subjected to UV light (270 nm, 22 mW cm^{-2}) for different time periods. The height of each gel was measured prior to and immediately after UV exposure.

In order to follow the course of the degradation in different media, 36 hydrogel pads (240 μL of prepolymerization solution each) were polymerized in a silicone mold for 2 min (360 nm, 6 mW cm^{-2}). After the gels had been swollen overnight in an excess of the media (media including phosphate saline buffer (DPBS), PR- and FCS-free DMEM, PR-containing and FCS-free

DMEM and FCS- and PR-containing DMEM, 9 replicates for each medium), their height was measured. The swollen hydrogels were thereupon degraded under UV light (270 nm, 22 mW cm^{-2}) for 1, 5, and 10 min (resulting in triplicates for each exposure time and each medium), and their height was again assessed immediately after the exposure using DSA 25 contact angle goniometer (Krüss, Germany). The gel composition (Figure 1C, yellow) was used for further experiments, named as Gel-N10 hydrogel (32.38 mmol L^{-1} PEGMA, 1.3 mmol L^{-1} PEGDMA and 0.13 mmol L^{-1} GelMA-low). As a negative control (Figure 1C, light blue), the analogous hydrogel composition without GelMA was used (32.38 mmol L^{-1} PEGMA, 1.3 mmol L^{-1} PEGDMA), named as Gel-N0 or GelMA-free PEGMA/PEGDMA hydrogel.

2.6. Cell Encapsulation and Long-Term Cultivation

NHDF (used between passage 6 and 8) and HeLa cells were suspended in either Gel-N0 or Gel-N10 precursor solutions with 0.3% (w/v) LAP. To reduce the harmful exposure of uncrosslinked PEGDMA and PEGMA monomers, cells were added last with a final cell density of 2.5×10^6 cells mL^{-1} , followed by immediate photocuring. Hydrogel formation and cell encapsulation were induced by exposure to long-wave UV light (360 nm, 6 mW cm^{-2} , 2 min) and performed in 8 well μ -slide (ibidi, Martinsried, Germany). Hydrogels had a volume of 200 μL and were covered with 200 μL DMEM after photopolymerization. Entrapped cells were cultured in DMEM with 10% FCS and 1% penicillin-streptomycin for 14 d (37 $^{\circ}\text{C}$, 5% CO_2). The cell culture medium was refreshed every 2–3 d.

2.7. UV Photodegradation

Cell-laden Gel-N10 hydrogel solutions were prepared as described previously in this section. Hydrogels were produced by casting 1 mL of the precursor solution against a Teflon mold (37.6 mm \times 13.8 mm \times 3 mm), followed by immediate photocuring. The hydrogel films were subsequently released from the Teflon mold, transferred into a Petri dish, and swollen overnight in DMEM. To ensure rapid UV photodegradation, FCS had to be removed using one of the following methods: a) exchanging DMEM against DPBS for 3 h; b) exchanging DMEM against FCS-free DMEM for 3 h; or c) swelling the hydrogels overnight in FCS-free DMEM. The photodegradation process was induced by irradiation at 270 nm for 10 min at 22 mW cm^{-2} . Patterning of the hydrogels was performed using a quartz-chromium photomask, the chromed parts of the photomask protected the cells in the hydrogel from UV-induced damage. After UV degradation, the hydrogels were transferred back into Petri dishes and cultured overnight in DMEM supplemented with FCS (37 $^{\circ}\text{C}$, 5% CO_2).

2.8. Live/Dead Staining

Cell viability of encapsulated NHDF and HeLa cells within the hydrogel was monitored using live/dead staining with calcein-AM and propidium iodide. Staining was performed after 1, 7, and 14 d of cultivation for NHDF and on day 1 postphotodegradation for HeLa cells. The supernatant cell culture medium was

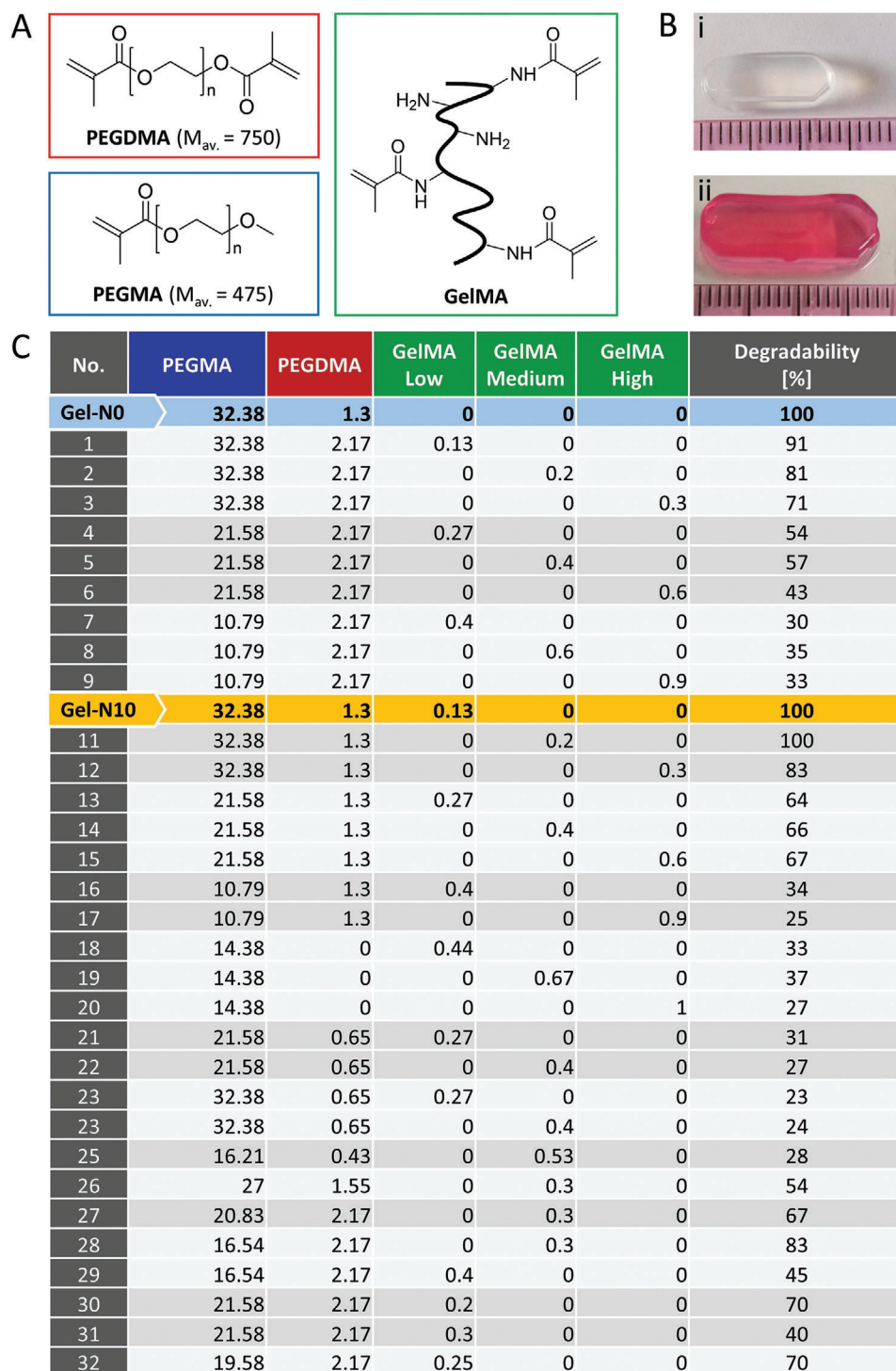


Figure 1. A) Chemical structure of monomers and crosslinker used in the construction of a combinatorial library. B) Photographs of an exemplary hydrogel (i) before swelling and (ii) after swelling in DMEM with scale. C) Combinatorial screening of hydrogel prepolymerization mixtures with regard to their photodegradability after hydrogel formation. For all further experiments were chosen Gel-N0 (light blue): GelMA-free negative control hydrogel; and Gel-N10 (yellow): GelMA-containing hydrogel. Entries are in mmol L⁻¹ prepolymerization mixture.

removed before hydrogels were stained with calcein-AM (4 ng mL⁻¹) and propidium iodide (20 ng mL⁻¹). The staining solution was removed after 20 min incubation. The hydrogels were then washed several times with DPBS and covered with DMEM. A confocal microscope (Leica TCS SPE DMI4000B, Leica Microsystems, Wetzlar, Germany) was used to visualize z-stacks of approximately 300 μm thickness (step size: 5 μm) per sample, which were converted into 3D images using Leica LAS X software.

2.9. PrestoBlue Proliferation Assay

PrestoBlue assay was performed to monitor cell survival and proliferation of HepG2 in Gel-N10 and Gel-N0 hydrogels over a period of 7 d. Cell-laden hydrogels of 200 μL volume were prepared as previously described in a 48-well plate and covered with 1 mL DMEM. Cell-free hydrogels served as corresponding blanks. Metabolic activity was measured 1-, 2-, 3-, and 7 d postencapsulation. For this purpose, the supernatant was removed, and hydrogels were washed with DPBS, followed by the addition of 300 μL PrestoBlue solution (DMEM/PrestoBlue = 9:1) and incubation for 5 h (37 °C, 5% CO₂). Afterwards, 100 μL supernatant of sample and blank, respectively, was transferred to a 96-well plate and fluorescence was measured (Ex/Em: 560 nm/600 nm, integration time: 400 ms) with a microplate spectrophotometer (SpectraMax ID3, Molecular Devices, San José, USA). Normalization was done by setting the initial fluorescence intensity at day 1 to 100% and dividing the measured intensities of day 2, 3, and 7 by the initial value.

2.10. MTT Cell Viability Assay

MTT cell viability assay was performed to determine the cytotoxicity of the photodegradation products of Gel-N10. HeLa cells were seeded at a density of 1 × 10⁴ cells per well in a 96-well plate and cultured overnight (37 °C, 5% CO₂). Then, the culture medium was removed, and cells were treated with the degradation products in different dilutions (nondiluted, 1:1, 1:2, 1:5, 1:10, 1:100, 1:1000). The degradation products were obtained by complete photodegradation of a Gel-N10 hydrogel, which was swollen in FCS-free DMEM overnight. The concentration of the undiluted sample was assessed at 53 mg mL⁻¹, resulting from the following equation, where w_i is the initial dry weight, V_{before} is the hydrogel volume before swelling and V_{after} is the volume after complete swelling.

$$c \left[\frac{\text{mg}}{\text{mL}} \right] = \frac{w_{\text{dry}}}{V_{\text{after}}} = \frac{m(\text{PEGMA}) + m(\text{PEGDMA}) + m(\text{GelMA}) + m(\text{LAP})}{V_{\text{before}} + \frac{\epsilon m}{\rho(\text{DMEM})}} \quad (2)$$

Live controls for each dilution were done by exchanging the medium without compound addition, but ensuring the same ratio of DMEM (FCS) to DMEM (FCS-free) as in the corresponding samples. After 72 h exposure, dead controls were treated with 5 μL Triton X-100 (20% (v/v)), followed by addition of 15 μL MTT solution to each well. The reaction was stopped after 3 h of incubation by adding 100 μL lysis buffer. Absorption was measured at

595 nm with a microplate spectrophotometer (SpectraMax ID3, Molecular Devices, San José, USA) the next day. A viability of 100% was assigned to the live controls. Average cell viability and standard deviation were calculated from $n = 3$ with respect to live and dead controls.

2.11. Data Analysis and Statistics

Data analysis and statistics were carried out using Origin-Pro 2020. All data are presented as mean ± standard deviation (SD). Unless stated otherwise, the value of n is defined as the number of repeat attempts performed. A two-sample independent Student's *t*-test was conducted when two average values were compared. If more average values needed to be compared, one-way analysis of variance (ANOVA) with Bonferroni correction was carried out across groups. In all cases, significance was defined as $p < 0.05$ (* $p < 0.05$, ** $p < 0.01$, and *** $p < 0.001$).

3. Results and Discussion

Three factors influence the non-degradability of polymerized GelMA under 270 nm UV light on a reasonable timescale: 1) reduced swellability of polymerized GelMA; 2) amide-bound methacrylates less prone to photomediated scission; and 3) the presence of aromatic UV-absorbing amino acids. Therefore, we aimed to identify a gelatin-containing PEG-composite hydrogel that, while still being cell-friendly, could be degraded in under 10 min; we took this timeframe as a benchmark for convenient handling (if longer time is used, the samples were overheated). Through combinatorial synthesis, we systematically examined the dependence of several factors (i.e., amount of crosslinker, amount of monomers, and degree of monomer methacrylation) on photodegradability. To map the structure–function relationship of each hydrogel composition and its degradability, we prepared a combinatorial library of GelMA-containing hydrogels. We varied the degree of GelMA methacrylation (20–35%, 50–60%, and 80–90% methacrylation, respectively defined as GelMA-low, medium, and high, see Figure S2B, Supporting Information), its concentration in the prepolymerization mixture, and the concentration of PEGMA and PEGDMA for a total of 32 unique combinations (combinatorial library see Figure 1). Crosslinking reactions and hydrogel formation were achieved via photopolymerization at 360 nm at a lower intensity (6 mW cm⁻²), benefiting from the noncontact, on-demand nature of polymerization and its biocompatibility. These characteristics will be important in subjecting the hit-composition to cell viability experiments. After photopolymerization in a silicone mold, hydrogel pads were allowed to swell in deionized water for 24 h; pad dimensions were altered due to swelling (Figure 1B). GelMA is known to reduce the swelling rate, hence why the swelling factor differed for each composition. Next, hydrogel pads were subjected to UV light (270 nm, 10 min, 22 mW cm⁻²). Each hydrogel mass was measured before degradation and after removing the liquid degradation products. The degradation ability was determined as follows:

degradation ability

$$= \frac{m(\text{before degradation}) - m(\text{after degradation})}{m(\text{before degradation})} \quad (3)$$

The degradation ability ranged from completely degradable within 10 min (100% degradability) to only partially degradable (25%). Upon comparing gel compositions 1–3 with compositions 10–12, the proportion of bifunctional crosslinker PEGDMA declined 1.64-fold, leading to increased degradability for all GelMA functionalization degrees due to greater swellability. The degradability of GelMA-low- and medium-containing gels thus shifted from 91% resp. 81% to complete degradability (100%). The correlations were identified for lower PEGMA concentrations with respect to water: a 1.64-fold reduction in crosslinker concentration led to an increase in degradability from 51% on average (gels 4–6) to 66% on average (gels 13–15). However, further dividing the crosslinker concentration by two resulted in reduced degradation, halving the degradation ability from 65% on average (gels 13 and 14) to 29% on average (gels 21 and 22) under the same PEGMA concentration.

The more GelMA was added, the worse the degradation behavior was (Figure 1C, entries 4, 30, and 31). When using the same amounts of PEGMA and PEGDMA, 70% degradation was achieved with 1.88% GelMA-low with respect to water (gel 30). Adding 1.35-fold more GelMA-low reduced the degradation to 54% (gel 4) and adding 1.5-fold GelMA-low slashed the degradation rate nearly twofold to 40% (gel 31).

Mathematic approximation was applied to map structure-function relationships. Absolute molar amounts of methacrylate moieties in PEGMA, PEGDMA, and in GelMA with different functionalization degrees were used as input (x_1 to x_5 , corresponding to PEGMA, PEGDMA, GelMA-low, GelMA-medium, and GelMA-high, respectively). The degradation ability was assessed as described earlier, expressed as a percentage, and taken as an output variable. A multivariant square model without bilinear terms according to

$$y_{\text{approx}} = a^T x \quad (4)$$

with

$$a^T = (a_1, \dots, a_{11}) \quad (5)$$

$$x^T = (1, x_1, x_2, x_3, x_4, x_5, x_1^2, x_2^2, x_3^2, x_4^2, x_5^2) \quad (6)$$

was adapted for mathematical approximation, in which the ordinary least squares method was used. Overall 29 combinations, a mean error of degradation ability $\sum_{(i)} |y_i - y_{\text{approx},i}|$ resulted in 6.6%, rendering the model reliable. This approximation resulted in the following quadratic equation for degradability (%), where n denotes the absolute amount of methacrylated moieties:

$$\begin{aligned} \text{Degradability} = & 115.82 + 35.26A + 194.35 B - 4763.23 C \\ & - 3308.41 D - 2252.01 E - 3.48 A^2 - 259.21 B^2 \\ & + 29725.71 C^2 + 14385.01 D^2 + 6447.94 E^2 \end{aligned} \quad (7)$$

$A = n(\text{PEGMA})$, $B = n(\text{PEGDMA})$, $C = n(\text{GelMA-low})$, $D = n(\text{GelMA-medium})$, and $E = n(\text{GelMA-high})$; substance amounts in μmol per 240 μL of prepolymerization mixture.

This equation confirms that adding any kind of GelMA to the prepolymerization mixture compromises degradation behavior,

if applied to the following concentrations: $C < 0.15$, $D < 0.23$, and $E < 0.35$ (all tested compositions fell within these ranges).

The model also reveals the clear effect of the degree of GelMA functionalization on degradability. Specifically, GelMA-high influenced degradation most negatively, followed by GelMA-medium and GelMA-low. This finding aligns with GelMA-low exhibiting the best swelling behavior, followed by GelMA-medium and GelMA-high.^[26]

Gel-N10 (32.38 mmol L⁻¹ PEGMA, 1.3 mmol L⁻¹ PEGDMA and 0.13 mmol L⁻¹ GelMA-low) showed one of the highest degrees of degradability (i.e., completely degradable after 10 min UV irradiation) given more than twofold swelling after 24 h (from 5 mm × 13 mm × 4 mm to 7 mm × 18 mm × 5 mm). Therefore, this hydrogel composition was subjected to further biological experiments.

A pure PEGMA/PEGDMA hydrogel exposes no bioactive sites and is therefore unsuitable for cell encapsulation. Supplementation with gelatin, offering Arg-Gly-Asp (RGD) sequences and matrix metalloproteinase (MMP) cleavage sites, promotes cell adherence and spreading within the hydrogel network. Conversely, combinatorial screening revealed the negative impact of GelMA on photodegradability, allowing the GelMA concentration to be as low as 1.25% (w/v) with respect to water in order to render the hydrogel completely photodegradable within 10 min. We tested whether supplementing PEGMA/PEGDMA hydrogel with only 1.25% (w/v) GelMA-low would increase the suitability of this hydrogel formulation for cell encapsulation. The biocompatibility and cell viability of NHDF were tested for Gel-N10 hydrogel and for the analogous GelMA-free PEGMA/PEGDMA hydrogel (Gel-N0), which served as a negative control. Whereas cells encapsulated in Gel-N0 hydrogels showed low viability (Figure 2A) and cell accumulation (Figure 2Biii) as expected due to the lack of adhesion sites, the composite Gel-N10 hydrogel displayed a homogenous cell distribution (Figure 2Bii) and advanced biocompatibility for at least 14 days upon photopolymerization (Figure 2A) along with cell spreading (Figure 2Bi). Additionally, proliferation of encapsulated HepG2 cells was monitored over a period of 7 days by PrestoBlue assay (Figure 2C). While metabolic activity remained nearly constant and slightly increased at day 7 for Gel-N10, a continuous decline in fluorescence was observed for the Gel-N0, resulting in a 90% decrease when comparing day 1 with day 7.

The combinatorial screening resulted in a hydrogel composition that balances two counteracting forces and combines the advantageous properties of both: the strong encapsulation properties of GelMA and favorable UV degradability of PEGMA.

Since the chosen cell medium (DMEM) contains UV-absorbing components (e.g., fetal calf serum [FCS] and phenol red [PR], see Figure S4, Supporting Information), which could reduce the effective UV intensity required for complete hydrogel degradation, we assessed their influence on the degradation behavior of Gel-N10. In this experiment, Gel-N10 was swollen in five liquids: 1) phosphate saline buffer (DPBS); 2) PR- and FCS-free DMEM; 3) PR-containing and FCS-free DMEM; 4) FCS-containing and PR-free DMEM; and 5) FCS- and PR-containing DMEM (Figure 3A,B). The Gel-N10 swollen in DPBS was completely degraded after 5 min irradiation. Although the presence of PR slightly slowed complete degradation, the full degradation of gels swollen in PR-free DMEM was reached after 10 min,

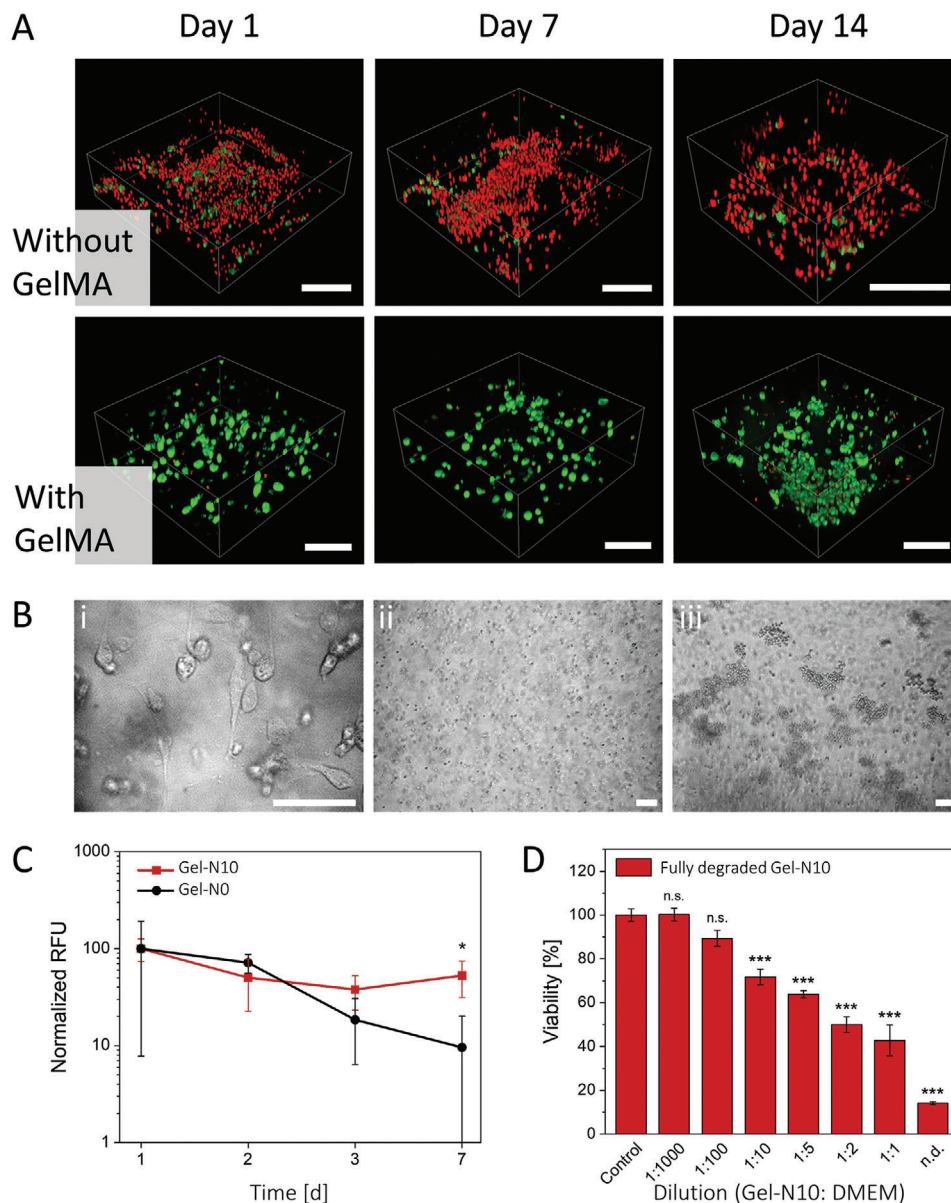


Figure 2. A) Live/dead staining of normal human dermal fibroblasts (NHDF) with calcein-AM (green, live cells) and propidium iodide (red, dead cells) embedded in GelMA-free PEGMA/PEGDMA (Gel-N0) and GelMA-containing (Gel-N10) hydrogels on day 1, 7, 14 postencapsulation, followed by imaging with confocal microscopy (Leica TCS SPE, scale bar: 200 μm). B-i) NHDF embedded in Gel-N10 hydrogels on day 1 postencapsulation. Comparison of HepG2 cells encapsulated in (ii) Gel-N10 and (iii) Gel-N0 hydrogels (scale bar: 100 μm). C) Proliferation behavior of encapsulated HepG2 cells in Gel-N10 and Gel-N0 hydrogels over a period of 7 d assessed by PrestoBlue assay ($n = 3$). D) Toxicity evaluation of Gel-N10 photodegradation products by MTT proliferation assay with HeLa cells after 72 h exposure ($n = 3$). The concentration of nondiluted degradation products was 53 mg mL^{-1} . Data are presented as mean \pm SD and statistically evaluated by (C) Student's t-test and (D) one-way ANOVA. *, **, *** represent $p < 0.05$, 0.01, and 0.001, respectively.

similar to Gel-N10 swollen in DPBS. Gel-N10 swollen in FCS-free-PR-containing and FCS- and PR-containing DMEM was completely degraded after ca. 34 and 80 min accordingly, since the UV-absorbing components deprived most of the incoming UV light, which is in accordance with the presence of UV-absorbing components (see also Figure S4 in the Supporting Information). Furthermore, PR bleaching was observed prior to gel degradation. We also investigated the degradation of Gel-N10 of

different thicknesses swollen in FCS-free DMEM and recorded the reduction degree in gel thickness with increasing UV illumination time, which was shown to be independent of the starting thickness (Figure 3C,D). As anticipated, FCS containing a mixture of proteins and as the major component of DMEM (10%) significantly reduced the degradation ability of Gel-N10 from 100% to about 60% after 10 min of UV exposure, with slightly worse degradation when combined with PR (Figure 3A,B and Figure

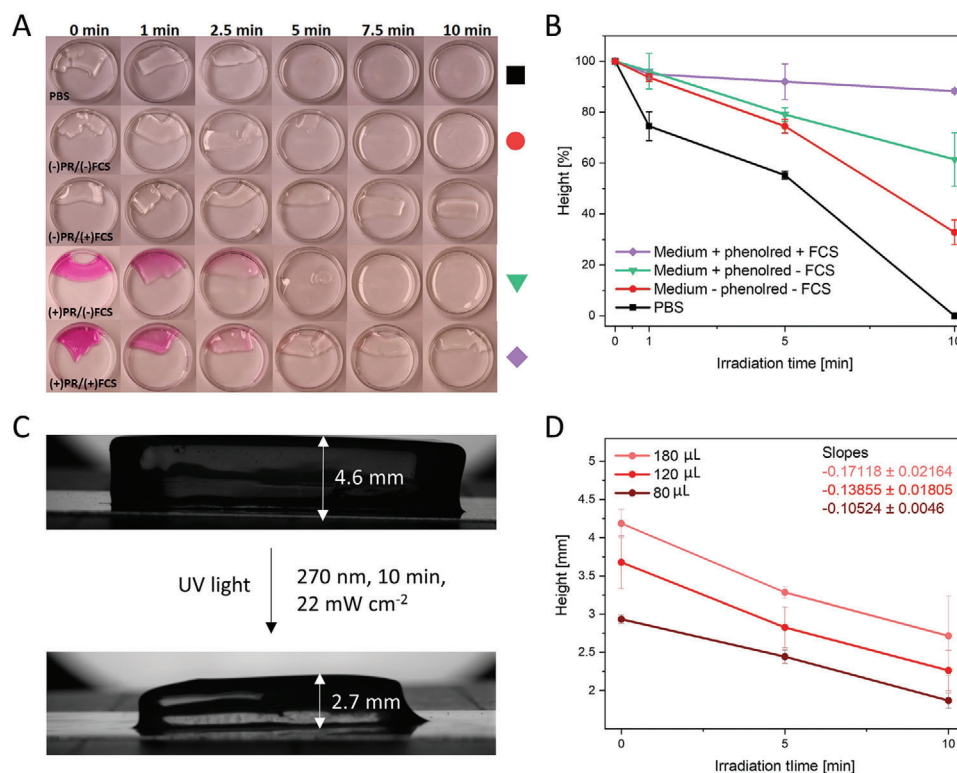


Figure 3. A) Photograph depicting degradation behavior at different time points of Gel-N10 swollen in PBS and in different PR-/FCS-containing/-lacking media. PR bleaching occurred within UV irradiation period, indicated by color shift from violet to colorless. B) Quantification of gel degradation of Gel-N10 swollen in PBS (black) and in different PR-/FCS-containing/-lacking DMEM (-PR, -FCS: red; +PR, -FCS: green; +PR, +FCS: lilac). C) Photograph depicting degradation behavior of Gel-N10 swollen in FCS-free DMEM after 10 min UV irradiation. D) Quantification of gel degradation of Gel-N10 swollen in FCS-free and PR-free DMEM, indicating the dependence of gel thickness on irradiation time, for three different starting thicknesses. Data are presented as mean \pm SD. Error bars are based on SD of three repetitions in two independent experiments.

S4, Supporting Information). Therefore, FCS must be eliminated prior to degradation to maintain a reasonable degradation time.

We further examined cell viability upon FCS removal and evaluated three strategies (Figure 4). After cell-laden gels were incubated overnight in FCS-containing DMEM (Figure 4a), DMEM was exchanged against DPBS for 3 h (Figure 4b), which resulted in reduced cell viability because cells were not supplied with any nutrients during this period. DMEM exchange against FCS-free DMEM manifested as high cell viability despite the absence of growth factors for 3 h (Figure 4g).

Incubating cell-laden gels overnight in FCS-free DMEM yielded similar viability despite the absence of growth factors for 1 day (Figure 4d). Cells covered with chromed parts of the photomask upon exposure to the UV light showed high viability (Figure 4e,h). Cells that were directly exposed to the UV light through transparent parts of the photomask were sacrificed through extensive washing immediately upon irradiation.

After UV irradiation of a Gel-N10 cell-containing hydrogel layer through a photomask, an array of free-standing hydrogel pads was obtained (Figure 5A,B), which could be used for the convenient production of arrayed matrices for 3D cell cultures.

The black areas of the photomask prevent photodegradation of the hydrogel and enable spatial control over degradation. The cells, which were not exposed to UV light due to coverage by

chrome parts of the photomask, were not affected by UV light and exhibited high viability (Figure 4e,h). Depending on the gel thickness, different illumination times may be needed to degrade the gel completely (see also Figure 3D). We also performed a toxicity evaluation of Gel-N10 photodegradation products by an MTT proliferation assay with HeLa cells (Figure 2D). For this, Gel-N10 hydrogels without cells were polymerized, swollen, and degraded by exposure to UV light (270 nm, 22 mW cm⁻², 10 min). The concentration of degradation products was determined to be 53 mg mL⁻¹. HeLa cells were then treated with the solution of degradation products at varying dilutions (1:1–1:1000) and incubated for 72 h. The MTT test revealed the inhibitory effect of undiluted degradation products on cell proliferation, which, however, decreased with increasing dilution (Figure 2D). Importantly, during the degradation of hydrogel, exposure of encapsulated cells to the degradation solution only occurred if degradation products were diffused into the nondegraded areas of the hydrogel, thus predominantly affecting cells at the edges. Since the hydrogels were placed in an excess of culture medium immediately after photodegradation, the degradation products were quickly removed from the hydrogel. Therefore, we assume that the effective concentration was low, and the duration of exposure was short. As shown in Figure 4e,h, we did not observe any significant impact of the photodegradation products on cells embedded in the Gel-N10 hydrogel.

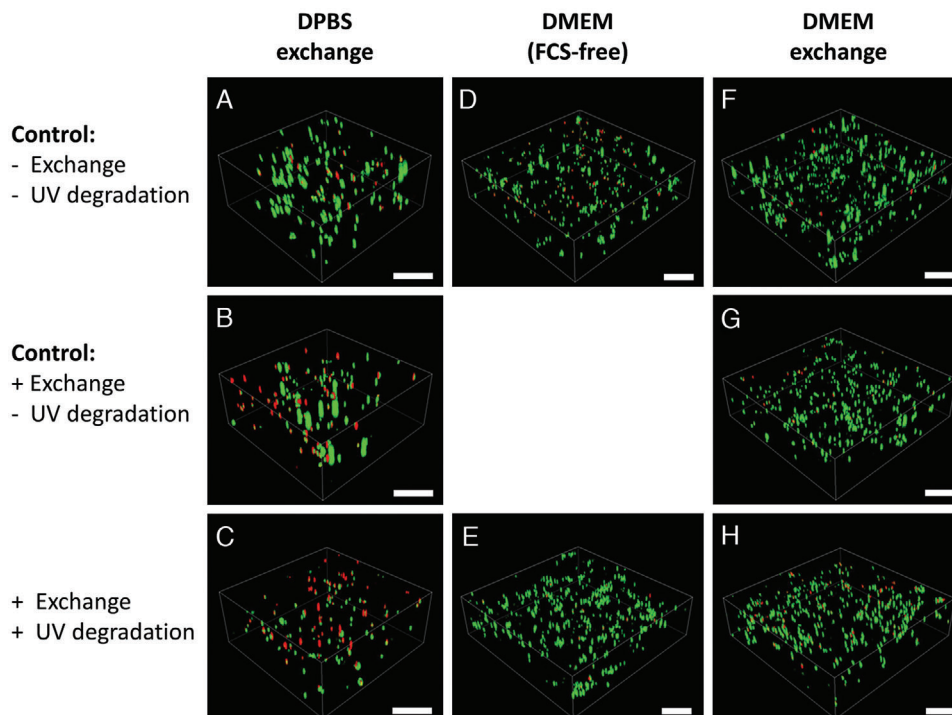


Figure 4. Comparison of three different approaches for transient FCS removal to ensure fast photodegradability of Gel-N10 hydrogels. The success of each strategy was evaluated by live/dead staining of HeLa cells at different time points: A,D,F) postencapsulation; B,G) after cell culture medium exchange; C,E,H) after photopatterning. Displayed HeLa cells were covered with chromed parts of the photomask and stained with calcein-AM (green, live cells) and propidium iodide (red, dead cells), followed by imaging via confocal microscopy (Leica TCS SPE; scale bar: 200 μ m).

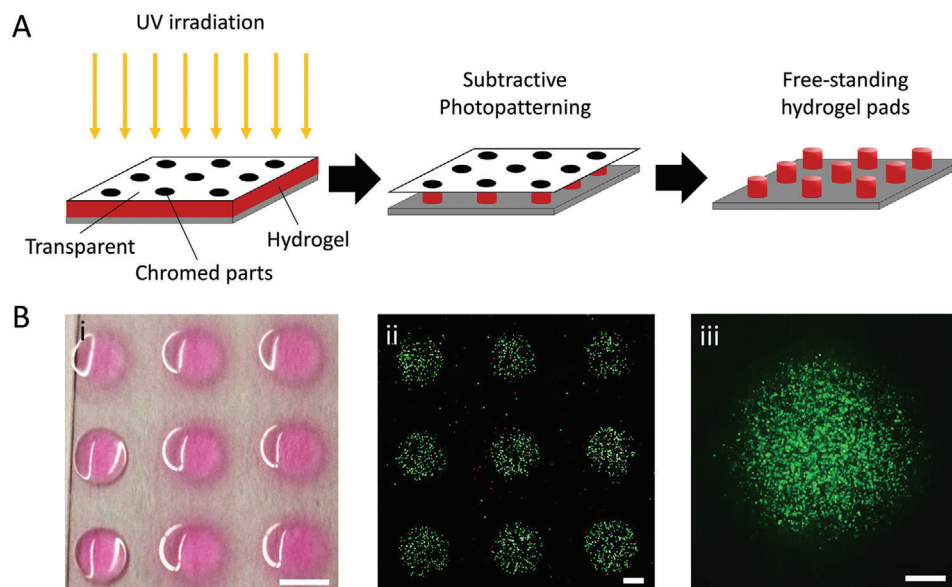


Figure 5. A) Schematic of on-demand Gel-N10 hydrogel micropad array production. B) Free-standing hydrogel pads of various sizes incorporating HeLa cells, prepared by photodegradation of Gel-N10 through a photomask of corresponding spot size (scale bar: 1 mm): (i,ii) 0.5 mm thick hydrogel, 1.5 min UV; (iii) 4.5 mm thick hydrogel, 10 min UV; (ii,iii) live/dead staining with calcein-AM (green, live cells) and propidium iodide (red, dead cells).

Essentially, we have developed a novel cell-friendly gelatin-based hydrogel that can be photodegraded on demand under cell-compatible conditions without the installation of photolabile groups prior to degradation.

4. Conclusions

Recently, we established a class of inherently photodegradable methacrylate-based hydrogels that were unsuitable for cell encapsulation despite being nontoxic. Gelatin-methacryloyl

represents a commonly used hydrogel for cell encapsulation; however, it exerts a manifold negative impact on photodegradation properties when added to an initially photodegradable hydrogel. To address this contradiction, a combinatorial screening of composite GelMA/PEGMA/PEGDMA-based photodegradable hydrogels was performed in this study. Testing revealed a hydrogel that is suitable for cell photoencapsulation and can be degraded at a rate of 0.1 to 0.2 mm min⁻¹, resulting in complete degradation of a hydrogel micropad, having the size of approx. 600 μm³ within 10 min. The procedure enables photopolymerization and photodegradation, benefiting from the noncontaminant and adjustable nature of light, and does not require modification of any of the monomers with photolabile groups. Polymerization, swelling, and subsequent photodegradation using a photomask have several advantages over using a photomask already at the stage of photopolymerization. First, photodegradation being delayed in time from the polymerization offers flexibility in experimental design (e.g., first a hydrogel layer, then an array of hydrogel micropads), whereas using the photomask already during the photopolymerization determines the geometrical form of the hydrogel from the very beginning. In addition, if the hydrogels are allowed to swell after polymerization, the photodegradation leads to stable features. This avoids the swelling-induced distortion of the features in hydrogels produced by photopolymerization using a photomask. Furthermore, the synthetic character of methacrylates enables finetuning of hydrogel properties, thus encouraging miniaturized combinatorial screening of hydrogels to ensure rapid adjustment for specific applications. The approach described herein could be useful in applications of photoresponsive and biocompatible materials (e.g., as sacrificial layers to mirror vascular systems), micrometer-scale cell-laden hydrogel particles for modular biofabrication, and responsive bimodal hydrogel systems.

Supporting Information

Supporting Information is available from the Wiley Online Library or from the author.

Acknowledgements

This project was partly supported by DFG (Heisenbergprofessor Projektnummer: 406232485, LE 2936/9-1). Furthermore, the authors thank the Helmholtz Program “Materials Systems Engineering”. This research was funded by the DFG (German Research Foundation) under Germany's Excellence Strategy 2082/1-390761711 (Excellence Cluster “3D Matter Made to Order”) and by the Bundesministerium für Bildung und Forschung under the KMU-NetC funding measure (3D-Bio-Net, FKZ 03VNE1034D). The authors also thank Maxi Hoffmann for the help with rheology experiments, supported by the Stiftung der deutschen Wirtschaft (SDW) within the Klaus Murmann fellowship. T.G. was funded by a Kekulé Fellowship of the Chemical Industry Fund. M.K. thanks the Carl Zeiss Foundation for financial support.

Open access funding enabled and organized by Projekt DEAL.

Conflict of Interest

The authors declare no conflict of interest.

Data Availability Statement

The data that supports the findings of this study are available in the Supporting Information of this article.

Keywords

gelatin-methacryloyl, hydrogels, poly(ethylene glycol) methacrylate, photodegradation, screening

Received: April 1, 2021

Revised: May 17, 2021

Published online:

- [1] L. M. Johnson, B. D. Fairbanks, K. S. Anseth, C. N. Bowman, *Biomacromolecules* **2009**, *10*, 3114.
- [2] K. T. Nguyen, J. L. West, *Biomaterials* **2002**, *23*, 4307.
- [3] L. Li, J. M. Scheiger, T. Tronser, C. Long, K. Demir, C. L. Wilson, M. A. Kuzina, P. A. Levkin, *Adv. Funct. Mater.* **2019**, *29*, 1902906.
- [4] P. Gupta, K. Vermani, S. Garg, *Drug Discovery Today* **2002**, *7*, 569.
- [5] S. Matsumoto, S. Yamaguchi, S. Ueno, H. Komatsu, M. Ikeda, K. Ishizuka, Y. Iko, K. V. Tabata, H. Aoki, S. Ito, H. Noji, I. Hamachi, *Chem. - Eur. J.* **2008**, *14*, 3977.
- [6] R. V. Ulijn, *J. Mater. Chem.* **2006**, *16*, 2217.
- [7] D. Schmaljohann, *Adv. Drug Delivery Rev.* **2006**, *58*, 1655.
- [8] Q. Wu, L. Wang, H. Yu, J. Wang, Z. Chen, *Chem. Rev.* **2011**, *111*, 7855.
- [9] L. Li, J. M. Scheiger, P. A. Levkin, *Adv. Mater.* **2019**, *31*, 1807333.
- [10] A. M. Kloxin, A. M. Kasko, C. N. Salinas, K. S. Anseth, *Science* **2009**, *324*, 59.
- [11] C. Siltanen, D.-S. Shin, J. Sutcliffe, A. Revzin, *Angew. Chem., Int. Ed.* **2013**, *52*, 9224.
- [12] A. M. Rosales, S. L. Vega, F. W. DelRio, J. A. Burdick, K. S. Anseth, *Angew. Chem., Int. Ed.* **2017**, *56*, 12132.
- [13] I. Tomatsu, K. Peng, A. Kros, *Adv. Drug Delivery Rev.* **2011**, *63*, 1257.
- [14] M. A. Azagarsamy, D. D. McKinnon, D. L. Alge, K. S. Anseth, *ACS Macro Lett.* **2014**, *3*, 515.
- [15] B. D. Fairbanks, S. P. Singh, C. N. Bowman, K. S. Anseth, *Macromolecules* **2011**, *44*, 2444.
- [16] T. L. Rapp, C. B. Highley, B. C. Manor, J. A. Burdick, I. J. Dmochowski, *Chem. - Eur. J.* **2018**, *24*, 2328.
- [17] V. X. Truong, K. M. Tsang, G. P. Simon, R. L. Boyd, R. A. Evans, H. Thissen, J. S. Forsythe, *Biomacromolecules* **2015**, *16*, 2246.
- [18] F. Yanagawa, S. Sugiura, T. Takagi, K. Sumaru, G. Camci-Unal, A. Patel, A. Khademhosseini, T. Kanamori, *Adv. Healthcare Mater.* **2015**, *4*, 246.
- [19] B. A. Mann, K. Kremer, C. Holm, *Macromol. Symp.* **2006**, *237*, 90.
- [20] J. A. Benton, C. A. DeForest, V. Vivekanandan, K. S. Anseth, *Tissue Eng., Part A* **2009**, *15*, 3221.
- [21] K. Yue, G. Trujillo-de Santiago, M. M. Alvarez, A. Tamayol, N. Annabi, A. Khademhosseini, *Biomaterials* **2015**, *73*, 254.
- [22] J. W. Nichol, S. T. Koshy, H. Bae, C. M. Hwang, S. Yamanlar, A. Khademhosseini, *Biomaterials* **2010**, *31*, 5536.
- [23] A. I. Van Den Bulcke, B. Bogdanov, N. De Rooze, E. H. Schacht, M. Cornelissen, H. Berghmans, *Biomacromolecules* **2000**, *1*, 31.
- [24] C. B. Hutson, J. W. Nichol, H. Aubin, H. Bae, S. Yamanlar, S. Al-Haque, S. T. Koshy, A. Khademhosseini, *Tissue Eng., Part A* **2011**, *17*, 1713.
- [25] R. Kale, A. Bajaj, *J. Young Pharm.* **2010**, *2*, 90.
- [26] H. Yoon, S. Shin, J. Cha, S.-H. Lee, J.-H. Kim, J. T. Do, H. Song, H. Bae, *PLoS One* **2016**, *11*, e0163902.